Progress report of the AEgIS experiment (2019)

The AEgIS/AD-6 collaboration

As a detailed report [1] outlining the long term physics goals and related work for AEgIS has recently been submitted to the SPSC, this progress report will concentrate only on the physics results achieved in 2019, and in particular on the work with positrons and positronium.

The AEgIS experiment [2] has the goal of measuring the behaviour of antimatter in the Earth's gravitational field. The experimental protocol is based on the pulsed production of a beam of antihydrogen atoms, launched horizontally, and measuring the gravity-induced vertical displacement of ground-state antihydrogen atoms by means of a position-sensitive detection device based on gratings and a high-spatial resolution detector. Pulsed formation of antihydrogen is based on the charge exchange process:

$$Ps^* + \bar{p} \rightarrow \bar{H}^* + e^- \tag{1}$$

A crucial figure of merit for the measurement is N_{det}, the number of atoms reaching the detector; the divergence of the formed beam is determined by the temperature (and space charge) of the antiprotons, and the efficiency of the beam formation mechanism. Furthermore, for identical divergence, reaching higher sensitivity greatly benefits from lower velocities.

In the last four years, AEgIS has worked towards validating the steps required for the pulsed formation of Rydberg antihydrogen atoms, and has achieved this goal at the end of 2018 [3]. In 2019, in the absence of antiprotons, we have focused on working with positrons and positronium, relying on one hand on measurements carried out in 2018 within the 1T cryostat, and on the other hand on the dedicated external positronium test setup.

CERN-SPSC-2020-002 / SPSC-SR-265
14/01/2020

Optimisation of the e^+ to Ps converter

In 2018, we had developed a high-resolution position-sensitive detector for slow positronium [4]. The detection scheme is based on the photo-ionization of positronium in a magnetic field and the imaging of the freed positrons with a Microchannel Plate assembly. The spatial resolution of the detector is around 100 μm.

This detector has allowed for [5]:

- a spatially precise and rapid monitoring of Ps emission into vacuum from our e^+ to Ps converter in the cryogenic, 1T $\bar{H}$ production region,
- the monitoring of the Ps laser excitation to the intermediate n=3 and to the Rydberg levels used for $\bar{H}$ production via charge exchange (eq. (1)),
- a characterization of the velocity distribution of Ps emitted by our e^+ to Ps converters in the cryogenic, 1T region. A most probable velocity of Ps of $\sim 1.7 \cdot 10^5$ m/s (in agreement with previous measurements in a similar converter [6, 7]) has been found.

The charge exchange cross section is expected to strongly depend on the Ps velocity. In particular, any reduction of the Ps velocity will beneficially affect the cross section [8]. For this reason, in 2019 we have performed an optimization of the characteristics of the e^+ to Ps converter with the goal of increasing the amount of emitted Ps and minimizing its velocity.

e^+ to Ps converters with different nanochannel size and length with respect to the target used in the first $\bar{H}$ formation via charge exchange in 2018 [3] have been produced [9]. The emission of Ps from the converters has been studied via Single Shot Positron Annihilation Lifetime Spectroscopy (SSPLAS) [10]. In figure 1, we show (in the inset) the SSPALS spectrum measured in a e^+ to Ps converter (with a positron implantation energy of 3.3 keV) compared to a spectrum with a target without Ps formation. Both spectra show a prompt peak given by the prompt e^+ annihilations in the respective targets while the e^+ to Ps converter shows a strong excess at delayed timed corresponding to Ps self-annihilation after emission from the converter target into the vacuum. The difference between the two spectra (Ps signal) corresponds to the fraction of Ps emitted from the converter and is shown in the main panel of the same figure. In samples with nanochannels of around 8-14 nm diameter and length of $\sim 1\mu$m (sample A), an emission of $\sim 35\%$ of implanted e^+ as Ps has been observed, while in converters with the same nanochannel size and shorter length (400 nm) the Ps emission amounts to ~ 41 % (sample B).

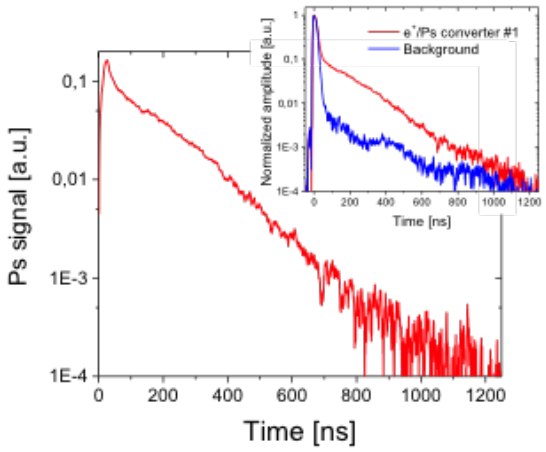

Figure 1. Difference of two SSPALS spectra (Ps signal) measured for sample A and for a target without Ps formation. The two SSPALS spectra are shown in the inset.

The velocity of Ps emitted by the converters has been estimated by measuring the width of the $1^3S \rightarrow 2^3P$ transition line. A 243 nm UV laser pulse (700 μJ energy) has been used to excite Ps from 1^3S to 2^3P. Ps on this level is then selectively photo-ionized with a 532 nm laser pulse. The effect of the photo-ionization is visible as a reduction of delayed Ps annihilation with respect to the case in which no lasers fire. An example of photo-ionization signal in SSPALS measurements is shown in Fig. 2 for sample A.

The fraction of Ps excited to the 2^3P level (and subsequently photo-ionized) can then be estimated as the difference of the areas below the two SSPALS spectra (with laser on and off), normalized on the area below the SSPALS spectrum with laser off. This normalized difference is usually called S(%) parameter and, in the present measurements, has been estimated for the time interval between 50 and 550 ns from the positron prompt peak. The $1^3S \rightarrow 2^3P$ transition line has been explored by measuring the S(%) parameter as a function of the UV wavelength. The line shape for Ps emitted from sample A and measured with a prompt-peak-laser pulse delay of 25 ns is shown in Fig. 3.

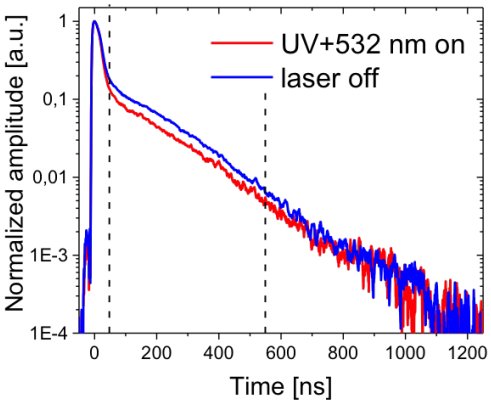

Figure 2. SSPALS spectra of Ps into vacuum (emitted by sample A) with laser off (blue curve) and UV+IR lasers (243.01 nm+ 532 nm) fired around 25 ns after positrons are injected into the converter (red curve) are shown. Each spectrum is the average of 40 single shots. The vertical dashed lines mark the area between 50 and 550 ns from the prompt peak used to evaluate the S(%) parameter (see text).

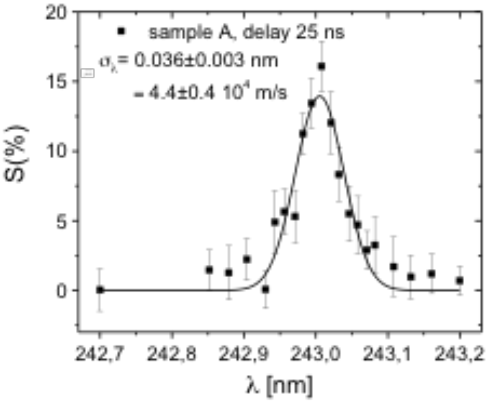

Figure 3. $1^3S \rightarrow 2^3P$ transition line shape for Ps emitted from sample A. The transition line has been measured at with a laser delay of 25 ns from positron implantation. The measurements were performed by implanting positrons with an energy of 3.3 keV. In these measurements, an UV energy of 700 μJ was used. The solid line is a Gaussian fit.

The experimental data are fit to S(%)=A $\exp(\frac{-(\lambda-\lambda_0)^2}{2\sigma_\lambda^2})$, where σ_λ and λ_0 are the Gaussian width and the resonance wavelength respectively. The width of the peak is dominated by Doppler broadening and it can therefore be used to infer the Ps velocity spread in the direction of the UV laser. More specifically, the Ps velocity is related to σ_λ by the relation $\sigma_\lambda/\lambda_0 = \sqrt{\frac{<v_x^2>}{c^2}}$. According to this measurement, the average velocity of Ps emitted by sample A is $4.4 \pm 0.4 \cdot 10^4$ m/s. This velocity is around a factor 2 lower than the one observed in the target used in 2018. According to [8], this gives an enhancement of the cross section for the $\bar{H}$ production charge exchange reaction of up to a factor 6. In addition, the sample used for $\bar{H}$ production in 2018

had a Ps emission probability of the order of 7 % of implanted e^+ (mainly due to thermal treatment issues). The present sample A promises to guarantee a Ps emission probability in the 1 T field of around 3 times more. As a consequence, the total $\bar{H}$ production rate is expected to be enhanced of a factor 18 (3 x 6) only thanks to the use of the present, optimized converter. Naturally, additional independent enhancements in the $\bar{H}$ production rate are also expected (target and electrode layout, allowing the use of more highly excited states of Ps; increased numbers of antiprotons, thanks to the ELENA upgrade to the AD), while others are still under development, such as a lower divergence Rydberg positronium source (see below).

Efficient 2^3S positronium production by stimulated decay from the 3^3P level

We have recently demonstrated the production of a 2^3S Ps source via single-photon excitation of 1^3S to 3^3P with a subsequent radiative decay to 2^3S in an electric field [11] and in the absence of an electric field [7]. This last method in particular showed that it is possible to build an almost monochromatic 2^3S Ps source with a selected and tuneable velocity distribution in the 10^4 m/s range, with an overall efficiency between 0.7% and 1.4%, depending on the selected velocity [7].

After the end of the antiproton beam time in 2018, and in the beginning of 2019, we investigated experimentally the possibility of enhancing the production of 2^3S positronium atoms by simultaneously driving the $1^3\mathrm{S} \rightarrow 3^3\mathrm{P}$ and $3^3\mathrm{P} \rightarrow 2^3\mathrm{S}$ transitions, thus overcoming the natural branching ratio limitation of spontaneous decay from 3^3P to 2^3S. The decay of 3^3P positronium atoms toward the 2^3S level was efficiently stimulated by a 1312.2 nm broadband IR laser pulse. The dependence of the stimulating transition efficiency on the intensity of the IR pulse has been measured to find the optimal enhancement conditions. Fig. 4 shows the relative enhancement at long times after the e^+ injection time (t=0) for both spontaneous (grey) and stimulated (black) decays from the 3^3P state into the metastable 2^3S state ($\tau \sim 1.1\mu$s). A maximum relative increase by a factor of (3.1 $\pm$ 1.0) in the 2^3S production efficiency, with respect to the case in which only spontaneous decay is present, was obtained [12].

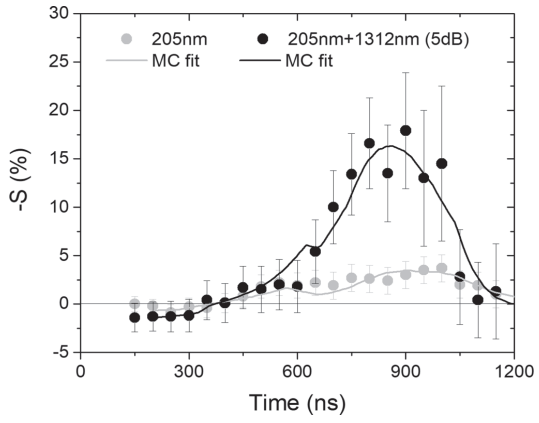

Figure 4. The experimental S[%] distribution measured with empirically determined optimal 1312.2 nm laser intensity, compared to the same distribution without the IR stimulation laser.

This measurement was carried out with a single common optical parametric generation stage for the UV and IR frequencies; a laser system with independent UV and IR laser lines (having independent nonlinear optical generation and amplification stages), is currently being prepared

in order to take full advantage of this $1^3S \rightarrow 3^3P2^3S$ stimulated excitation scheme in view of future measurements on a beam 2^3S Ps.

Further work with Ps and outlook for 2020

Two further areas of development were pursued in 2019: on one hand, preparatory work for laser-manipulating ground-state o-Ps (by repeatedly stimulating the 1^3S3^3P transition, where the lifetime of the 3^3P is around 2 ns) was carried out. And on the other, given the progress on the efficient formation of the meta-stable 2^3S state, we also focused on producing and detecting a (collimated) beam of Ps, both as a proxy for tests of the interaction of (Rydberg) $\bar{H}$ atoms with gratings, as well as an independent system with its own physics interests.

In the first case, the existing 243 nm UV laser produces short pulses ($\sim$ 1.5 ns); a further dye laser was adapted in 2019 to produce much longer ($\sim$ 25 ns) laser pulses at the same wavelength and instantaneous intensity, allowing multiple $1^3S \leftrightarrow 3^3P$ transitions for the same positronium atom. Together with the characterisation of the Ps velocity distribution as developed earlier and that relies on the existing laser system to produce both a 243 nm UV laser pulse used to excite Ps from 1^3S to 2^3P and the photo-ionization pulse with a 532 nm laser pulse (or alternatively a 205.2 nm pulse for $1^3S \rightarrow 3^3P$, followed by an IR photo-ionisation pulse at 1064 nm), we are now in a position to manipulate and characterize the formed Ps in view of reducing the divergence of the resulting expanding cloud. In the second half of the year, a further Alexandrite-based laser system (currently being refurbished) should allow extending the interaction time from 25 ns to $\sim$ 100 ns.

In a parallel development to the efficient formation of the meta-stable 2^3S state, the geometry of the test set-up was modified to allow a fraction of the formed metastable Ps to reach a cylindrical flight tube (essentially collimating a $\sim 2\pi$ source close to the origin, and thus allowing forming a "beam" of meta-stable 2^3S atoms. The first successful attempts of 2019 will be followed up in the coming months, in view of having a well-characterised "beam" with which to investigate both prototype gratings (a first iteration of the production technique for these was carried out at PSI in 2019) as well as high-resolution spatial detectors (both photo-ionisation as well as annihilation detectors).

[1] CERN-SPSC-2019-043; SPSC-P-334-ADD-1 (http://cds.cern.ch/record/2692828)
[2] CERN-SPSC-2007-017 ; SPSC-P-334 (http://cds.cern.ch/record/1037532)
[3] S. Aghion et al., (AEgIS Collaboration), "Pulsed production of antihydrogen", subm. to Nature Physics
[4] C. Amsler et al., (AEgIS collaboration), "A $\sim$100 μm-resolution position-sensitive detector for slow positronium" NIMB 457, 44 (2019)
[5] M. Antonello et al., (AEgIS collaboration), "Rydberg-positronium velocity and self-ionization studies in 1T magnetic field and cryogenic environment", in preparation
[6] S. Aghion et al., (AEgIS collaboration), "Laser excitation of the n=3 level of positronium for antihydrogen production" Phys. Rev. A 94, 012507 (2016)
[7] C. Amsler et al., (AEgIS collaboration), "Velocity-selected production of 2^3S metastable positronium", Phys. Rev. A 99, 033405 (2019)
[8] D. Krasnicky, R. Caravita, C. Canali and G. Testera, "Cross section for Rydberg antihydrogen production via charge exchange between Rydberg positroniums and antiprotons in a magnetic field", Phys. Rev. A 94, 022714 (2016)
[9] S. Mariazzi, P.Bettotti, S. Larcheri, L. Toniutti, R.S. Brusa, "High positronium yield and emission into the vacuum from oxidized tunable nanochannels in silicon", Phys. Rev. B 81, 235418 (2010)
[10] S. Aghion et al., (AEgIS collaboration), "Positron bunching and electrostatic transport system for the production and emission of dense positronium clouds into vacuum", NIMB 362, 86 (2015)
[11] S. Aghion et al. (AEgIS Collaboration), "Producing long-lived 2^3S positronium via 3^3P laser excitation in magnetic and electric fields", Phys. Rev. A 98, 013402 (2018)
[12] M. Antonello et al., (AEgIS collaboration), "Efficient 2^3S positronium production by stimulated decay from the 3^3P level", Phys. Rev. A100, 063414 (2019)